Journal of Magnetic Resonance 243 (2014) 8–16

Contents lists available at ScienceDirect

Journal of Magnetic Resonance

journal homepage: www.elsevier.com/locate/jmr

Optimized multiple-quantum filter for robust selective excitation of metabolite signals

Mirjam Holbach [a,*], Jörg Lambert [b], Dieter Suter [a]

[a] Experimental Physics III, TU Dortmund University, 44227 Dortmund, Germany
[b] Leibniz-Institut für Analytische Wissenschaften, ISAS e.V., 44139 Dortmund, Germany

ARTICLE INFO

Article history:
Received 25 November 2013
Revised 30 January 2014
Available online 19 March 2014

Keywords:
SSel-MQC
Lactate editing
Optimal control
Robust pulses
MRS

ABSTRACT

The selective excitation of metabolite signals *in vivo* requires the use of specially adapted pulse techniques, in particular when the signals are weak and the resonances overlap with those of unwanted molecules. Several pulse sequences have been proposed for this spectral editing task. However, their performance is strongly degraded by unavoidable experimental imperfections. Here, we show that optimal control theory can be used to generate pulses and sequences that perform almost ideally over a range of rf field strengths and frequency offsets that can be chosen according to the specifics of the spectrometer or scanner being used. We demonstrate this scheme by applying it to lactate editing. In addition to the robust excitation, we also have designed the pulses to minimize the signal of unwanted molecular species.

1. Introduction

In vivo ^{1}H-MRS spectra of mammalian brain tissue contain information about ≈20 metabolites resonating in a very narrow chemical shift range. The majority of the metabolite signals appear between 1.2 and 4.4 ppm [1]. This leads to considerable signal overlap, which is most severe for signals from coupled spins and from molecules whose concentrations are small. In addition macromolecules and lipids overlap with the metabolite signals. As an example, the lactate methyl resonance at 1.3 ppm can be obscured by a broad lipid peak. Unambiguous detection of metabolite signals *in vivo,* therefore, often requires selective excitation techniques.

Selective detection of metabolite signals can be achieved by spectral editing techniques that use differences in the scalar couplings to simplify the spectra [1]. Widely used methods are J-difference editing [2–5] and multiple-quantum-filters (MQF). While J-difference editing requires two scans that are subtracted, multiple-quantum-filter sequences allow spectral editing in a single scan and, therefore, reduce artifacts, e.g. from motion of the patient.

Many *in vivo* studies require absolute quantification of metabolite signals related to a disease or disorder. In these studies, co-edited or poorly suppressed undesired signals that contribute to the measured signal distort the real value of the desired metabolite concentration. Therefore, improved selective excitation techniques are desirable that allow reliable quantification.

Early work on the detection, quantification and imaging of lactate *in vivo* based on double quantum coherence transfer was reported e.g. in [6,7]. Single-shot lactate editing and simultaneous lipid suppression is also possible with a zero-quantum-filter, as described in [8]. Here we investigate the performance of multiple-quantum filters using the example of the sequence Sel-MQC from He et al. [9]. Current work on the basis of this sequence can be found e.g. in [10–19]. Pickup et al. developed a robust method for generating lactate maps *in vivo* in selected regions with a sequence that is a combination of the Sel-MQC technique with longitudinal Hadamard slice selection and chemical shift imaging [10]. In [11] the clinical feasibility of this technique was demonstrated. On the basis of the sequence in [10] early and patient-specific markers of therapeutic response in cancer treatment can be monitored [12,13]. The Sel-MQC sequence was also combined with fast spectroscopic imaging methods like spiral MRSI [14] or multi-spin-echo-readout [15]. Enhancement of *in vivo* lactate signal was achieved by a refocused version of the sequence [16] or in combination with binomial spectral-selective pulses [17]. A variant of the sequence for relaxation measurements was developed in [18].

In spite of these improvements, selective excitation with multiple quantum filters in the presence of experimental non-idealities like field inhomogeneities is challenging for low concentrated metabolites with overlapping signals. In general B_1-inhomogeneity in high field MRI systems and also at clinical field strengths poses

* Corresponding author.
E-mail address: mirjam.holbach@tu-dortmund.de (M. Holbach).

http://dx.doi.org/10.1016/j.jmr.2014.03.007
1090-7807/

one of the major problems for *in vivo* measurements. It is known that the performance of MQF sequences degrades rapidly in inhomogeneous magnetic fields [9,16]. Especially in the *evolution period* where double quantum coherences are manipulated by radio-frequency (RF) pulses, imperfect flip angles or off-resonance conditions have a significant effect on the outcome of the sequence. This may result in severe signal loss of the edited signal or in suboptimal selectivity, e.g. inefficient suppression of unwanted signals. As under *in vivo* conditions and in MRI-scanners the B_1- and B_0-inhomogeneities are much larger than in NMR-systems the poor performance of multiple-quantum filters is very critical and may prohibit lactate editing with this method in large volumes with considerable field inhomogeneities and for relatively small lactate concentrations. The unwanted co-excitation of the metabolites alanine or threonine may be a problem for an unambiguous lactate quantification. To avoid these problems small volumes and preferably homogeneous B_1- and B_0-fields can be used. As an example Melkus et al. [15] used a 17.6 T animal scanner with a small birdcage resonator. Several mechanisms can cause lactate signal loss in lactate editing sequences. 'NMR-invisible lactate' is one problem that was reported recently in [19] but was also observed previously e.g. in [20]. It seems that this phenomenon is associated with binding of the lactate molecule to large molecules which involves a change of the T_2-relaxation time for the lactate and therefore a broadening in the line width.

The goal of this work is to develop and implement an improved spectral editing scheme that is robust against inhomogeneous fields and achieves selective excitation of the targeted metabolite over the relevant range of field strengths with minimal loss of signal. At the same time, it prevents co-editing of unwanted molecules and retains a small SAR value. In this study we chose lactate and alanine as an example system where lactate is the metabolite of interest and alanine should be suppressed. Alanine is also a critical metabolite, similar to lactate, e.g. for tumor studies. The method that we present here can also be applied to the other combinations of metabolites, such as the selective excitation of alanine and the suppression of lactate.

1.1. Pulse sequence

To investigate the performance of multiple quantum filter sequences for selective excitation of metabolite signals in the presence of B_1- and B_0-inhomogeneity, we have chosen here the Selective Multiple-Quantum-Coherence Transfer (SSel-MQC) sequence from He et al. [9]. Fig. 1 shows the pulse sequence, which achieves selective excitation of the lactate methyl resonance and suppresses all signals with different coupling topologies in a single scan. In particular, the large signal components from water and lipid are suppressed very effectively.

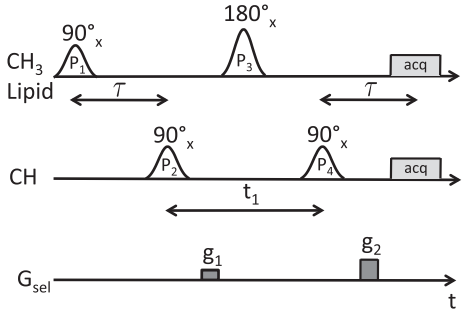

Fig. 1. Pulse sequence SSel-MQC [9]. The relative intensities of the selection gradients (G_{sel}) are $g_1 : g_2 = 1:2$. The pulses in the first row (P_1 and P_3) are selective for the lactate methyl and lipid resonances at 1.3 ppm, the pulses in the second row (P_2 ans P_4) excite the frequencies at 4.1 ppm (lactate methine group and water).

As shown in Fig. 1, the sequence uses selective pulses to excite the CH_3 and CH protons of lactate and consists of three periods. It starts with the *preparation period*, where the first 90°-pulse P_1 excites single-quantum coherence of the lactate methyl spins which evolves under chemical shift and J-coupling during the delay $\tau = \frac{1}{2J}$, where J = 6.9 Hz is the coupling constant between the lactate methyl and methine spins. At the end of this delay, the second 90°-pulse P_2 transforms the antiphase magnetization into double- and zero-quantum coherence. This conversion occurs only for the coupled spins that were excited by the two selective RF pulses. During the following *evolution period* (t_1), chemical shift and J-coupling are refocused by the inversion pulse P_3 while the gradient pulse g_1 labels the double quantum coherence. The last 90°-pulse P_4 initiates the *detection period* by converting the double quantum coherence back into single quantum coherence. The second gradient pulse g_2 has twice the area of g_1 to select coherence that was converted from double to single quantum while dephasing all other (unwanted) signal contributions.

1.2. Optimal control

Improving the performance of the pulse sequence and reducing the effect of experimental imperfections can be achieved by a number of approaches. Their theoretical basis is optimal control (OC) theory, which is a powerful method for steering complex dynamical systems in a desired way. The design and optimization of RF pulses is, therefore, a typical application. Recent work of different groups has shown that OC in NMR and MRI can increase the sensitivity of optimized experiments and make them robust against deviations in instrumental parameters, such as an inhomogeneous distribution of RF amplitudes. This is particularly important for *in vivo* MRI or MRS where OC allows one to design low-power RF pulses that are insensitive to offset and perform the targeted operation with high precision. Recent applications of OC pulse sequence design can be found in [21–23] for liquid NMR and in [24,25] for solid state NMR. In MRI and MRS early work includes [21,26–29] which demonstrated that the improved sequences are also useful under *in vivo* conditions. So far optimized broad bandwidth frequency selective pulses and flip angle homogenizing broadband pulses were developed in [26–28]. In [21,29] spatially selective pulses were optimized.

The use of OC for pulse design enables the optimization of RF pulse shapes that provide (a) the most efficient transfer of coherence from an initial spin state ρ_0 to a desired target spin state C (state-to-state) transfer or (b) a desired effective Hamiltonian [30]. Neglecting relaxation, the dynamics of a nuclear spin system can be described by the Liouville-von Neumann equation

$$\frac{d\rho(t)}{dt} = -i[H(t), \rho(t)] \tag{1}$$

with the Hamiltonian $H(t)$ and the density matrix $\rho(t)$. $H(t)$ can be written as

$$H(t) = H_0 + \sum_k \omega_{1k}(t) I_k, \tag{2}$$

where H_0 is the internal spin Hamiltonian and the second term describes the effect of the RF field. $\omega_{1k}(t)$ are the RF amplitudes coupling to the component I_k ($k = x, y$) of the nuclear spin.

OC is based on the optimization of a function of the type

$$J_j(\omega_{1k}) = \Phi_j - \lambda \int_0^T \sum_k \omega_{1k}^2(t) dt, \tag{3}$$

where Φ_j is the efficiency (the fidelity) to be maximized and the second term penalizes the deposited power scaled with the weighting factor λ, and T is the duration of the pulse.

If the system is to be steered from a given initial state ρ_0 to a final state ρ_D (state-to-state transfer), the efficiency can have the form

$$\Phi_1 = Tr(\rho_D \rho(T)). \quad (4)$$

In the more general case, where the pulse should implement a specific propagator U_D, the efficiency can be

$$\Phi_2 = |Tr(U_D^\dagger U(T))|^2. \quad (5)$$

The function in Eq. (3) has to be maximized in the space of possible pulse shapes ω_{1k} typically by numerical simulation and iterative optimization.

The majority of the OC applications used gradient-based optimization such as the gradient ascent pulse engineering (GRAPE) algorithm [22,29,26]. Here we use a Krotov-based OC approach that was recently implemented for NMR by Maximov et al. [30,31] and for MRI by Vinding et al. [21]. This method applies a sequential update rule where all controls are updated simultaneously. As shown in [31,21], this method can be faster per iteration especially for a large number of spins and the convergence behavior does not depend on the initial guess in contrast to gradient-based methods.

2. Pulse optimization

2.1. Goals

The pulse sequence SSel-MQC described in Section 1.1 acts as a multiple quantum filter for lactate methyl signals. The thermal equilibrium density operator of the lactate spins is $\rho_0 = I_z + F_z$, where $I_z = I_{1z}$ is the spin of the methine group and $F_z = I_{2z} + I_{3z} + I_{4z}$ denotes the three spins in the methyl group of lactate. For ideal pulses, the first CH_3-selective $\frac{\pi}{2}$-pulse (P_1 in Fig. 1) generates y-magnetization for the methyl spins: $\rho_1 = I_z - F_y$. The following delay $\tau = \frac{1}{2J}$ generates antiphase magnetization: $\rho_2 = I_z + 2I_zF_x$. Here we use a reference frame where the CH-spins are on resonance. The chemical shift evolution of the CH_3-spins will be refocused by the 180°-pulse P_3 and can, therefore, be neglected in ρ_2. The following pulse P_2 rotates the methine spin and creates zero- and double-quantum-coherences in $\rho_3 = -I_y - 2I_yF_x$. During the delay t_1, the gradient g_1 together with g_2 selects specific coherence pathways. The single-spin term I_y in ρ_3 does not pass through the MQF and will not be considered any further. The selective π-pulse P_3 refocuses couplings and chemical shift evolution during t_1 for the CH_3-spins. The last pulse (P_4) again creates antiphase magnetization of the CH_3-spins: $\rho_4 = -2I_zF_x$. During the final delay of duration τ, the magnetization refocuses to $\rho_5 = -0.5F_y$, which is detected.

In real experiments the RF pulses deviate from the ideal behavior assumed above. In particular, the amplitude of the RF field is inhomogeneous which results in variations of the flip angles throughout the region of interest. This effect is most severe in high-field MRI where the wavelength of the RF field becomes comparable to the size of the RF coil. In addition, B_0-inhomogeneity leads to a distribution of the resonance frequencies. These non-idealities generate additional terms that were not considered in the density operators ρ_i ($i = 2, \ldots, 5$). Non-ideal selective pulses also excite, e.g., the methyl group of alanine and generate signals similar to those of lactate. In the case of inhomogeneous B_1-fields, e.g., a 90°-pulse applied to I_z generates not only y-magnetization, but also some z-magnetization which is not suppressed by the MQ filter. Optimal control allows one to design pulses that achieve a more robust suppression of such undesired signal contributions.

In the following, we use optimal control theory to design pulses that are robust with respect to pulse imperfections and implement the desired transformations for lactate while simultaneously suppressing the unwanted alanine signal. Since the initial condition is well defined by thermal equilibrium, the excitation pulse P_1 can be designed as a state-to-state transfer that takes the thermal equilibrium state to the targeted state with y-magnetization of the lactate methyl group. Before application of the pulses P_2, P_3 and P_4, however, the spin system contains multi-spin terms which all must be transformed correctly by the pulses. At this point, it is, therefore, necessary to use pulses that implement the correct unitary transformation, i.e. universal rotation pulses. All three pulses were optimized for coupled spins taking into acount the whole spin system of the molecules.

2.2. Excitation pulse

The first pulse can be implemented as a state-to-state transfer. For the optimization, we consider two initial density operators for lactate and alanine:

$$\rho_{0,Mol} = I_{z,Mol} + F_{z,Mol},$$

where Mol = lac, ala.

The desired target operators for an ideal lactate CH_3-selective 90°-pulse are:

$$\rho_{D,lac} = I_{z,lac} - F_{y,lac},$$

$$\rho_{D,ala} = I_{z,ala} + F_{z,ala}.$$

We therefore searched for pulses that (i) maximize the overlap with these desired target operators (ii) minimize unwanted components, in particular transverse components I_x and I_y of lactate as well as alanine and (iii) minimize the pulse energy $\int_0^T \sum_k \omega_{1k}^2(t)dt$. The overlap between the targeted states and the actual states was calculated as

$$\Phi_{Mol} = \frac{Tr(\rho_{D,Mol}\rho_{Mol}(T))}{Tr(\rho_{D,Mol}\rho_{D,Mol})}, \quad (6)$$

where $\rho_{Mol}(T)$ is the actual state of the molecular subsystem at the end of the pulse.

2.3. Universal rotation pulses

The pulses P_2, P_3 and P_4 were optimized as universal rotation pulses. In the SSel-MQC sequence the pulses P_2 and P_4 should implement $(\pi/2)_x$ rotations on the CH-proton of lactate. At the same time, we use these pulses for suppressing the alanine signal by requiring that they do not affect the alanine spins. This effect can be achieved either by requiring that the pulses act as unit operators on the alanine spins or that each pulse inverts them. The second possibility led to better convergence in the optimization process. Accordingly, we used the following target propagators:

$$U_{D,lac}(P_2) = exp(-i\frac{\pi}{2}I_{x,lac}),$$
$$U_{D,ala}(P_2) = exp(-i\pi(I_{x,ala} + F_{x,ala})).$$

Pulse P_3 should refocus the methyl spins of the lactate. Again, we can improve the suppression of alanine by requiring that the alanine spins are not affected by P_3. We, therefore, used the target propagators

$$U_{D,lac}(P_3) = exp(-i\pi F_{x,lac})$$
$$U_{D,ala}(P_3) = \mathbf{1}$$

for optimizing P_3.

The fidelity of the universal rotation pulses was calculated as

$$\Phi_{Mol} = \frac{|\,Tr(U_{D,Mol}^\dagger U_{Mol}(T))|^2}{\left|Tr(U_{D,Mol}^\dagger U_{D,Mol})\right|^2}, \quad (7)$$

where $U_{Mol}(T)$ is the resulting propagator of the pulse for the respective molecular subsystem.

2.4. Robustness

One of the main goals of this work is to make the performance of the sequence robust: it should work well in the presence of experimental imperfections, in particular inhomogeneous B_1- and B_0 fields. To achieve this goal, we included the relevant parameter range in the design of the pulses and required high fidelity over the whole parameter range. The overlap Φ_{Mol} was evaluated at several points of the parameter range and the resulting fidelities were summed. For this study, we chose a parameter range of ±20% from the nominal B_1-field which is significantly larger than required for the NMR spectrometer where our experiments were performed but smaller than in a typical high-field MRI scanner. To make the pulse robust with respect to B_0 inhomogeneity, we also averaged over frequency shifts over a range of Δ = ±7 Hz. The value of 7 Hz was chosen to let the pulses still be selective, but robust over a range of B_0-offsets that meets the situation in some *in vivo* measurements.

2.5. Pulse shape optimization with optimal control

The calculation of the optimal control pulses in this work was realized using the Krotov-based algorithm described in [31,30]. The implementation was based on the Matlab-code provided by Maximov et al. in [30] which uses the formulation from Tannor et al. which is similar to the original Krotov formulation [30].

For our application, we extended the algorithm in two directions. First, we let the pulses act simultaneously on two different spinsystems - in our case the two metabolites lactate and alanine. Second, the algorithm was extended for the calculation of pulses that are robust over a range of RF field strengths and frequency offsets Δ as discussed in Section 2.4.

Pulses designed by optimal control theory can have highly variable, 'noise-like' shapes. If the hardware is not perfectly linear, this leads to distortions of the pulse shape and, therefore, reduced fidelity. This problem can be reduced significantly if the pulses are forced to be as smooth as possible. The smoothness is limited by other requirements, in particular the main goal of a high fidelity. To design smooth pulses, we adapted the procedure of Ref. [30]: at each iteration, the pulse was filtered and components far from resonance were suppressed. The resulting pulses were relatively smooth and the experimental performance corresponded quite well to the theoretically predicted behavior. As an additional bonus, the suppression of the non-resonant frequency components resulted in pulses with lower total energy corresponding to lower SAR values than pulses that were optimized without this additional condition. The resulting pulse shapes for the pulses P_1, P_2 and P_3 are displayed in Fig. 2.

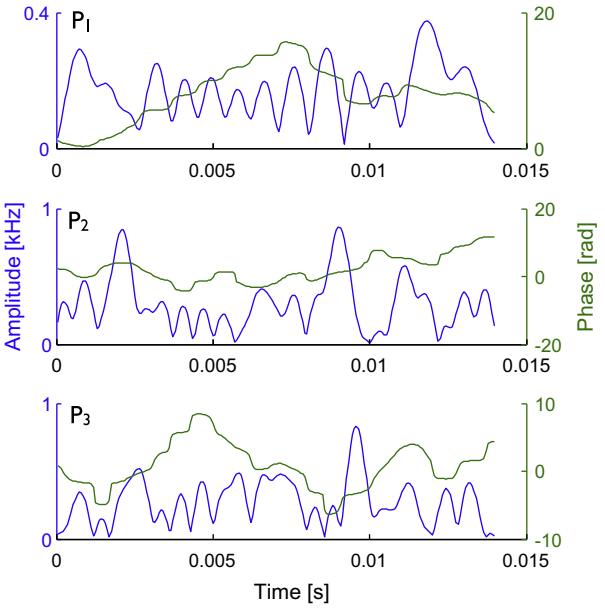

Fig. 2. Pulse shapes of the pulses P_1, P_2 and P_3.

3. Implementation and pulse performance

3.1. Experimental setup

For the experimental tests, we used NMR samples containing the metabolites lactate and alanine as well as a lipid. Lactate and alanine share the same spin system and have similar spectra. As a result the standard lactate editing sequence normally excites not only lactate but also alanine. We, therefore, have chosen this molecule as an example of an unwanted molecule whose signal should be suppressed. To distinguish the lactate from the co-edited alanine, we use a high-resolution NMR-spectrometer which distinguishes between these resonances on the basis of their different chemical shifts. Typically alanine resonates at higher field. The experimental data in this work were measured with a Bruker Avance II 500 MHz NMR-spectrometer using a Bruker QXI high resolution probehead and 5 mm sample tubes. Two samples were used, with the first containing lactate in D_2O (sample "lactate") and the second containing lactate, alanine and lipid in D_2O (sample "mixed"). For the lipid, we used sodium-lauryl-sulfate which resonates with a broad peak in the region around 1.3 ppm. Fig. 3 shows the spectrum of the mixed sample.

Performing the experiments in a high-resolution NMR-spectrometer combines the benefit of a very homogeneous B_0-field with a very homogeneous rf field compared to MRI-scanners. This allows us to study also the effect of RF inhomogeneity through systematic variation of the RF power of the pulses and the effect of B_0 inhomogeneity by variation of the frequency.

3.2. Robustness of excitation pulse

We first evaluate the performance of the excitation pulse P_1 which should implement a state-to-state transfer $F_z \rightarrow -F_y$ for

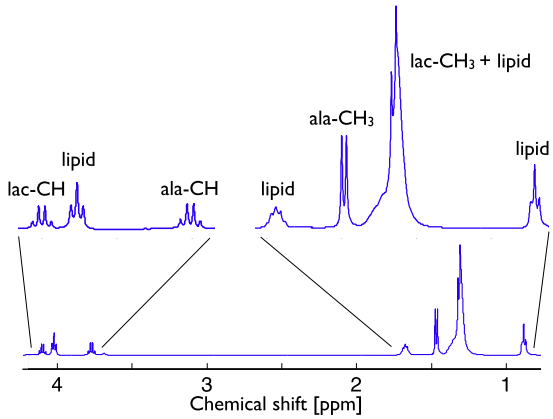

Fig. 3. NMR spectrum of the mixed sample containing D_2O, lactate, alanine and lipid, excited with a hard 90°-pulse. The alanine methyl group resonates at 1.47 ppm whereas the lactate methyl signal appears at 1.31 ppm overlapping with the broad lipid signal.

the methyl spins of the lactate while leaving all other spins unaffected. To differentiate between the lactate and alanine spins, we used the chemical shift difference of 75 Hz between the methyl resonances and chose a pulse duration of 14 ms to achieve good selectivity. The resulting pulse has a maximum RF amplitude of 376 Hz. The pulse was made robust over the range of RF field strengths from 80% to 120% of the nominal value and for frequency offsets Δ of ±7 Hz.

Fig. 4 shows the simulated performance of the optimized pulse and compares it to the performance of a standard Gaussian pulse with a duration of 11 ms whose frequency matches the resonance of the lactate methyl spins. In both cases, we plot the performance over a parameter range that is wider than the chosen optimization range: [0.5, 1.5] for the effective RF field strength in terms of the nominal value, and [−10,10] Hz for the frequency shift Δ. The plots show the efficiency

$$\Phi_{lac-CH_3} = \frac{Tr(\rho(T)F_{y,lac})}{Tr(F_{y,lac}F_{y,lac})},$$

with which the pulses generate transverse magnetization $F_{y,lac}$ when acting on the initial state $F_{z,lac}$. Fig. 4(a) shows that the performance of the Gaussian pulse is not robust with respect to inhomogeneities of RF and B_0 fields: The efficiency is only optimal (Φ_{lac-CH_3} = 1.0) for ideal B_0- and RF field strengths. Deviations from the ideal parameters produce a significant loss of efficiency, e.g. Φ_{lac-CH_3} = 0.6 at the edges of the profile where the RF field strength is 50% or 150%. Particularly for the RF amplitude this poses a major problem since the RF inhomogeneity of typical MRI scanners is at least of this order of magnitude. The efficiency profile along the parameter Δ is, of course, connected to the pulse length and can be adjusted to a certain extent.

In contrast to the Gaussian pulse, the optimized pulse excites y-magnetization over a broad range of parameters in an optimal way (Fig. 4(b)). The efficiency remains close to 1.0 and does not drop significantly over the parameter range that was chosen for the optimization. This range is marked by the gray rectangle in Fig. 4(b).

Also outside of the optimized region the signal loss is significantly lower than for the Gaussian pulse. For a direct comparison, Fig. 5 compares the efficiencies of both pulses as a function of the RF amplitude for Δ = 0 Hz, experimentally as well as theoretically. The improved excitation by the optimized pulse is clearly visible; over the range of ±20–30%, the fidelity remains very close to 1.0. The experimental data were measured with the lactate sample. They are in very good agreement with the simulation for the Gaussian pulse. In the case of the optimized pulse, the experimental data match the simulation over most of the parameter range but deviate slightly for higher RF amplitudes. The reason for this effect may be the more complicated pulse shape of the optimized pulse compared to the Gaussian pulse shape. Stronger modulations in the RF amplitudes during the pulse may cause transient effects which are more pronounced if the RF amplitude is scaled with a higher factor. Non-linearities of the amplifiers can lead to this effect and are more severe at high powers.

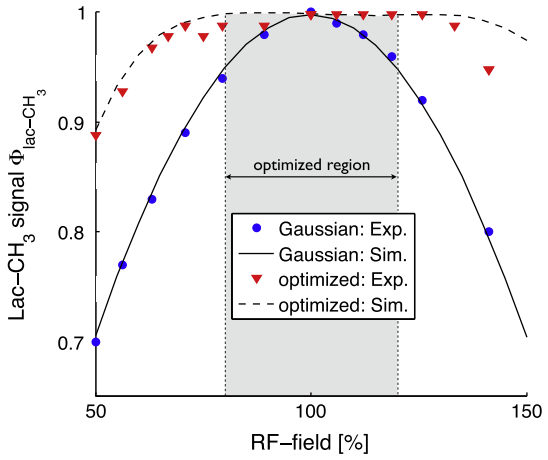

Fig. 5. Experimental and simulated data for the dependance of the Lac-CH_3 signal after a single Gaussian pulse and a single Krotov pulse on the RF amplitude. The measured points of the lactate sample represent the integrated Lac-CH_3 peak (y-magnetization). The displayed curves correspond to the cross-section of Figs. 4(a) and (b) respectively for an ideal B_0-field condition (Δ = 0 Hz). Differences between simulation and experiment of the optimized pulse may be due to transient effects distorting the strongly modulated pulse shape.

In addition to the robust excitation of the lactate methyl signal, the optimized pulse also suppresses the alanine signals in a robust way (efficiency profile not shown here). Only 1.3% of the alanine-CH_3 signal is left after the optimized pulse for ideal RF amplitude and B_0-field.

3.3. Universal rotation pulses

The refocusing pulse (P_3) and the multiple quantum excitation and detection pulses (P_2 and P_4) were realized as optimized universal rotation pulses with the same range of parameters for the robustness as for P_1. The optimized pulses show a very robust performance. The fidelity Φ_{lac} of P_2 and P_4, as defined in Eq. (7), has a mean value of 0.973 inside the optimized region. For the refocusing pulse P_3, the mean fidelity in the optimized region is 0.972.

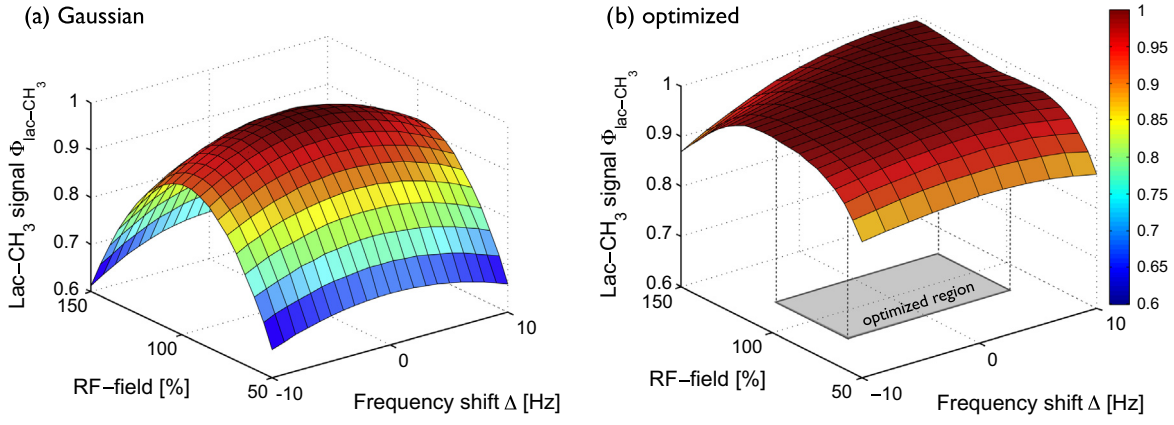

Fig. 4. (a) Efficiency profile of a single Gaussian 90° pulse (length: 11 ms) as a function of the RF field strength (100% corresponds to the nominal RF amplitude) and frequency shift Δ due to static field inhomogeneity. The plotted values denote the efficiency of the transfer $F_z \rightarrow -F_y$. (b) Efficiency profile of a single robust OC-pulse (first pulse in the sequence SSel-MQC). The efficiency of the lactate CH_3 excitation is robust over a range of field strengths.

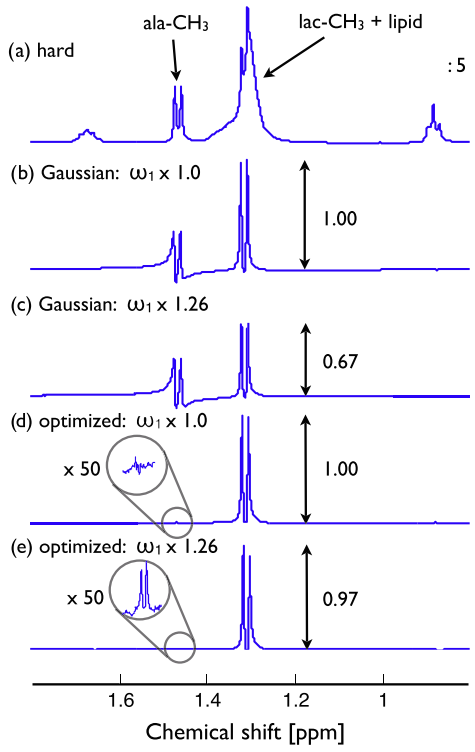

Fig. 6. Experimental spectra of the mixed sample containing lactate, alanine and lipid. (a) Reference spectrum obtained with a hard 90°-pulse; spectra (b)–(e) were obtained with the SSel-MQC sequence, using (b) Gaussian pulses and ideal RF amplitudes ω_1 (c) Gaussian pulses and non-ideal RF amplitudes (126%), (d) optimized pulses and ideal RF amplitudes, (e) optimized pulses and non-ideal RF amplitudes (126%).

4. Sequence performance

4.1. Lactate excitation

The pulse sequence SSel-MQC for lactate editing should excite the lactate methyl signal and at the same time suppress other unwanted signals. As shown in Fig. 6, the suppression of unwanted signals from uncoupled spins in water and lipids by the selection gradients G_{sel} works very well in a single scan: the lipid signals visible in the reference spectrum (a) are not present in spectra (b)–(e) which were obtained with the SSel-MQC sequence, and the same is true for the water resonance (not shown in the figure). In the spectrum in Fig. 6(d) the lipid signal is suppressed by a factor 450 compared to the spectrum in Fig. 6(a). In the case of the SSel-MQC sequence with Gaussian pulses (Fig. 6(b)), we find in addition to the lactate signal also a significant alanine signal. When the RF amplitudes are 26% higher than the optimal value, the lactate signal is reduced by 1/3, as shown in Fig. 6(c). This indicates that the Gaussian pulses are not robust with respect to RF inhomogeneity. The sequence with the optimized pulses, however, shows very robust performance as demonstrated by the last two spectra (Fig. 6(d) and (e)): with the nominal amplitude, as well as with amplitudes artificially increased by 26%, the editing sequence with optimized pulses suppresses the alanine resonances and the amplitude of the lactate signal remains almost at its maximum value. The alanine signal in the spectrum in Fig. 6(d) is suppressed by a factor 1200 compared to the spectrum in Fig. 6(a). This corresponds to a dynamic range of the filter of ≈62 dB.

The lactate signal excited by the SSel-MQC sequence reaches at most 50% of the lactate signal obtained with hard pulse excitation since the selection gradients refocus only one of the two coherence pathways. This value is found in the simulations as well as in the experiment for ideal pulses. However, as shown in Fig. 7(a), the resulting lactate-CH_3 signal decreases rapidly with deviations of the RF amplitude if the SSel-MQC sequence is implemented with Gaussian pulses. A miscalibration of ±50% of the RF amplitude results in a lactate-CH_3 amplitude of less than 0.1 (i.e. less than 20% of the ideal signal amplitude (= 0.5)). For an already very weak lactate signal in human tissue this poses a serious problem and can make the lactate detection impractical. If optimized pulses are used instead, their performance improves dramatically as shown in Fig. 7(b): In the optimized region a mean efficiency value of 98% is reached. In the whole displayed region in Fig. 7(b) the average efficiency is 86%.

Fig. 8 shows a direct comparison of the RF profiles for both sequences at zero frequency offset, $\Delta = 0$ Hz. The improved performance of SSel-MQC with optimized pulses can clearly be seen. The experimental data measured with the lactate sample are in very good agreement with the simulation for the sequence with Gaussian pulses. With optimized pulses the experimental data fit better for lower RF amplitudes. For higher RF amplitudes the measured data have still much higher values than the Gaussian version of the sequence. The deviations could, as mentioned above, originate from transient effects due to more complex RF amplitude envelopes. Here the influence of four pulses instead of one could explain a stronger deviation.

4.2. Co-editing

The use of spectral editing sequences for selective excitation of a desired metabolite may involve the problem of co-editing of another undesired metabolite that is also partly excited by the

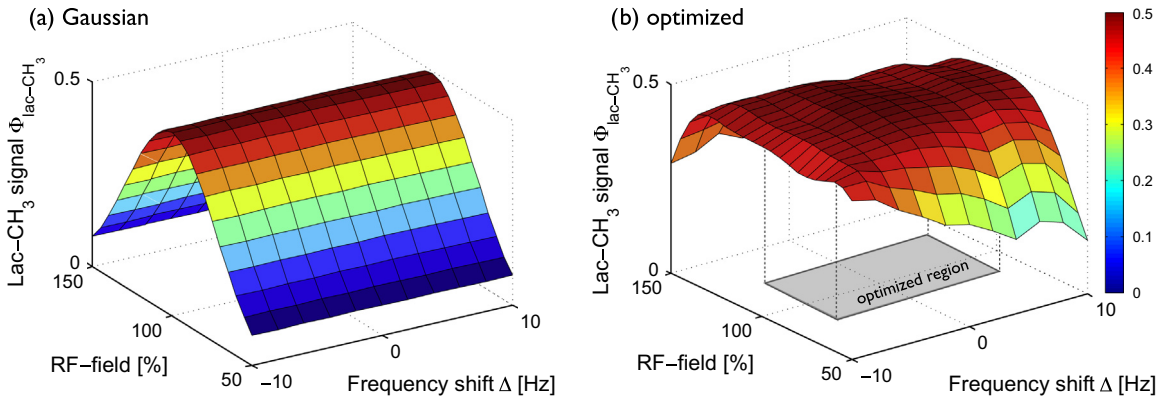

Fig. 7. Simulated efficiency profiles of lactate-CH_3 excitation by the SSel-MQC sequence as a function of the RF field strength (100% corresponds to the nominal RF amplitude) and frequency shift Δ due to static field inhomogeneity. (a) SSel-MQC with Gaussian pulses. Each pulse has a length of 5 ms. (b) SSel-MQC with optimized pulses.

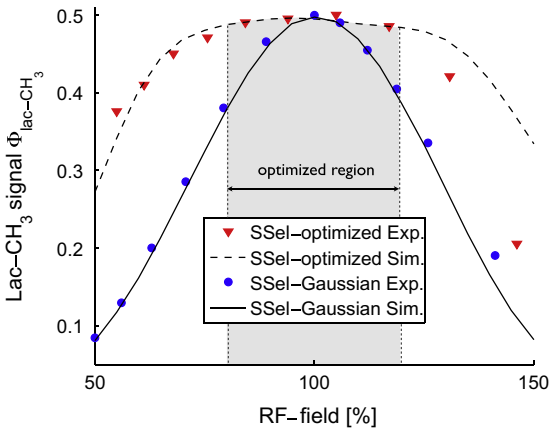

Fig. 8. Experimental and simulated data for the Lac-CH_3 signal after SSel-MQC as a function of the RF amplitude. The measured points correspond to the integral of the Lac-CH_3 peak (absolute magnetization). The displayed curves represent the cross-section of Figs. 7(a) and (b) respectively for an ideal B_0-field condition ($\Delta = 0$ Hz). The delay t_1 was set to 13 ms.

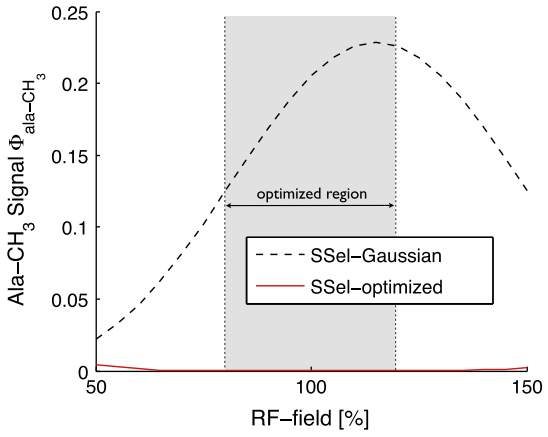

Fig. 10. Direct comparison of RF profiles for alanine co-editing. The curves represent cross-sections of the efficiency profiles in Fig. 9. Gaussian pulses result in co-editing of almost 50% of the maximal possible alanine signal. With the OC-version of the sequence, the co-edited signal stays below 1.0%.

editing sequence. In the case of a multiple-quantum-filter designed for lactate editing the co-excitation of alanine signals is possible due to the similar molecular structure. When standard selective pulses, as e.g. Gaussian pulses or sinc pulses, are employed, this feature is often not considered. In the literature lactate editing was e.g. in [16] performed using a multiple-quantum-filter with sinc-Gaussian pulses with a length of 5.5 ms and a bandwidth of 300 Hz. The simulated data in Fig. 9(a) show that with Gaussian pulses with a length of 5 ms, the sequence also excites a significant amount of alanine signal reaching up to 50% of the maximal possible value. In the case of overlapping signals or chemical shift selective imaging where only one data point is recorded for each voxel [32], this results in errors in the quantification of the lactate content. In contrast the editing sequence with optimized pulses produces a strong suppression of the alanine signals (see Fig. 9(b)). Almost no alanine signal is excited in the region of parameters displayed in the figure; Φ_{ala-CH_3} stays below 1.8% of the maximal possible alanine signal. The direct comparison of the RF profiles for $\Delta = 0$ Hz in Fig. 10 shows the advantage of the OC-version of SSel-MQC clearly: it suppresses the alanine signal very efficiently over the whole parameter range.

5. Discussion and conclusion

Selective *in vivo* measurements of metabolites with overlapping signals require spectral editing techniques, such as multiple quantum filters. However the performance of these sequences is far from optimal in the presence of experimental imperfections such as B_1- or B_0-inhomogeneities. For *in vivo* measurements and especially in high field MRI, B_1-inhomogeneity is one of the most challenging problems [33]. For small and overlapping signals this may impede their measurement. As a result, important information about the metabolism of the tissue or pathological situations is lost.

In this study, we used an optimal control approach to improve a multiple quantum filter sequence for spectral editing with the SSel-MQC [9] sequence for lactate editing in a single scan. The optimal control pulses were calculated with a Krotov-based algorithm described in [30]. In addition, we incorporated multiple optimization conditions: The pulses were optimized not only with respect to robust excitation of the targeted metabolite (lactate), but also to suppress unwanted molecules (in our example alanine). The pulses were designed to be robust over a range of RF amplitudes of ±20% and frequency offsets of ±7 Hz. For practical applications, the parameter range over which the sequence must be robust depends on the field strength and the RF coil system. Higher field MRI scanners may exhibit higher RF inhomogeneity and would require different pulses. A wider parameter range typically requires longer pulses with higher SAR values. A comparison between the relative SAR values of the optimized pulse P_3 and an adiabatic inversion pulse shows that in general the relative SAR values of the optimized pulses should be around 20–60% lower than values for the adiabatic pulses.

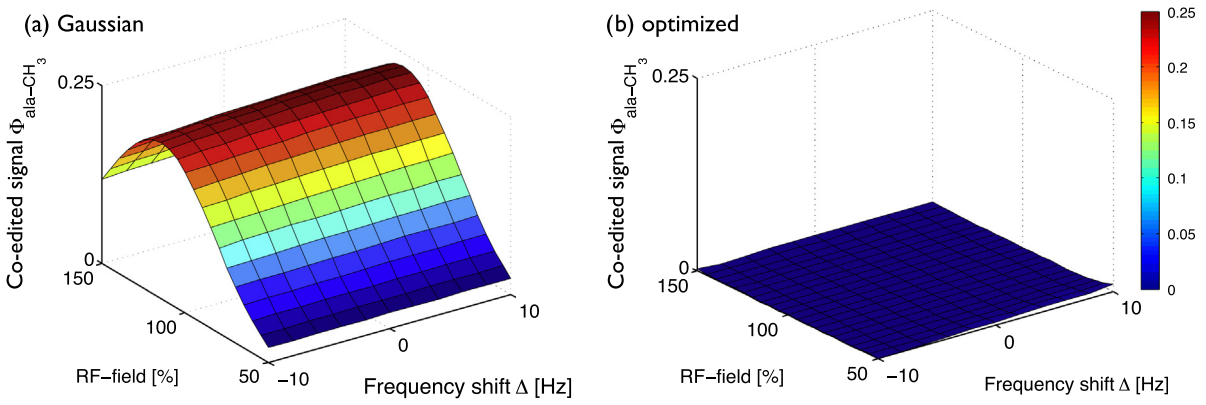

Fig. 9. (a) Alanine-CH_3 co-editing of the SSel-MQC sequence with four Gaussian pulses as a function of the RF field strength and frequency shift Δ corresponding to static field inhomogeneity. Each Gaussian pulse has a length of 5 ms. (b) Alanine-CH_3 co-editing after SSel-MQC sequence with optimized pulses.

The convergence of the optimization was largely independent of the initial guess for the pulse in accordance with previous work with this algorithm. In addition, we observed good convergence for state-to-state optimizations. However in the case of universal rotation pulses, we faced problems with numerical instabilities of the algorithm especially problems with convergence and loss of monotonicity. We found that for certain cases the convergence is better and were able to optimize the desired pulses with slight modifications as described in Section 2.3. Maybe these problems can be overcome by switching to the more general formulation of the algorithm described in [34,31] where additional parameters of the algorithm can be used to adjust the performance of the algorithm.

The performance of the optimized pulses was investigated by simulations and experiments. We applied the optimized editing sequence to a mixture of the metabolites lactate and alanine and added lipid to the sample to simulate *in vivo* conditions in which the lactate methyl signal overlaps with a broad lipid peak. We chose the metabolite alanine as an example for unwanted signals that should be suppressed but are co-edited by the standard editing sequences. The pulse performance was first tested with single pulses. Then the multiple quantum filter with optimized pulses was compared to the sequence with Gaussian pulses. The results show clearly that robust lactate excitation is possible over a relevant range of experimental parameters. Lipid suppression by the selection gradients works very well and the optimized version of the sequence achieves very robust alanine suppression. The suppression factors are 450 for the lipid signals and 1200 for the alanine signals.

In conclusion we were able to increase the measurable amount of lactate signal. This method works for signals losses due to B_1- and B_0-inhomogeneities. It has no influence on effects that cause line broadenings.

Another possible unwanted signal contribution to lactate edited images is threonine, which also has a resonance in the 1.3 ppm region of the spectrum and may be co-excited by a lactate MQ-filter. The principle of the method presented here can equally be applied to threonine.

The results of the NMR measurements in this work show that optimized spectral editing sequences allow one to reach an optimized editing performance in MRS measurements in inhomogeneous B_1- and B_0-fields. This permits the detection of lactate also in tissues with low lactate concentration for which standard methods are not sufficiently selective. Editing sequences with optimized pulses can also solve problems with overlapping and co-edited metabolite signals because undesired coherences can be suppressed. The reduced sensitivity of the targeted metabolite signal to RF inhomogeneity results in a more precise and unambiguous quantification of the chosen metabolite. The translation and application of the presented method to *in vivo* investigations is ongoing work and will be published in the future. This approach could also be extended to chemical shift selective imaging where signals of metabolites that have very similar chemical shifts cannot be separated by standard techniques because only one data point is recorded for each voxel. The presented principle was shown here for the example metabolites lactate and alanine but can equally be applied to mixtures of other metabolites.

Acknowledgment

The authors would like to offer their sincerest gratitude to Evangelisches Studienwerk Villigst for funding parts of this work.

References

[1] R.D. Graaf, D. Rothman, In vivo detection and quantification of scalar coupled 1 H NMR resonances, Concepts Magnet. Reson. 13 (1) (2001) 32–76.
[2] R.A. de Graaf, D.L. Rothman, Detection of γ-aminobutyric acid (GABA) by longitudinal scalar order difference editing, J. Magnet. Reson. 152 (1) (2001) 124–131.
[3] M.A. Smith, J.A. Koutcher, K.L. Zakian, J-difference lactate editing at 3.0 Tesla in the presence of strong lipids, J. Magnet. Reson. Imag. 28 (6) (2008) 1492–1498.
[4] C. Choi, N.J. Coupland, S. Kalra, P.P. Bhardwaj, N. Malykhin, P.S. Allen, Proton spectral editing for discrimination of lactate and threonine 1.31 ppm resonances in human brain *in vivo*, Magnet. Reson. Med. 56 (3) (2006) 660–665.
[5] H. Hetherington, J. Hamm, J. Pan, D. Rothman, R. Shulman, A fully localized 1H homonuclear editing sequence to observe lactate in human skeletal muscle after exercise, J. Magnet. Reson. (1969) 82. 1 (1989) 86–96.
[6] R. Hurd, D. Freeman, Metabolite specific proton magnetic resonance imaging, Proc. Natl. Acad. Sci. 86 (12) (1989) 4402–4406.
[7] R. Hurd, D. Freeman, Proton editing and imaging of lactate, NMR Biomed. 4 (2) (1991) 73–80.
[8] J.M. Star-Lack, D.M. Spielman, Zero-quantum filter offering single-shot lipid suppression and simultaneous detection of lactate, choline and creatine resonances, Magnet. Reson. Med. 46 (6) (2001) 1233–1237.
[9] Q. He, D.C. Shungu, P.C.M.V. Zijl, Z.M. Bhujwalla, J.D. Glickson, Single-scan *in vivo* lactate editing with complete lipid and water suppression by selective multiple-quantum-coherence transfer (Sel-MQC) with application to tumors, J. Magnet. Reson. 106 (1995) 203–211.
[10] S. Pickup, S. Lee, A. Mancuso, J. Glickson, Lactate imaging with Hadamard-encoded slice-selective multiple quantum coherence chemical shift imaging, Magnet. Reson. Med. 60 (2) (2008) 299–305.
[11] E.A. Mellon, S.-C. Lee, S. Pickup, S. Kim, S.C. Goldstein, T.F. Floyd, H. Poptani, E.J. Delikatny, R. Reddy, J.D. Glickson, Detection of lactate with a Hadamard slice selected, selective multiple quantum coherence, chemical shift imaging sequence (HDMD-SelMQC-CSI) on a clinical MRI scanner: application to tumors and muscle ischemia, Magnet. Reson. Med. 62 (6) (2009) 1404–1413.
[12] S.-C. Lee, M. Marzec, X. Liu, S. Wehrli, K. Kantekure, P.N. Ragunath, D.S. Nelson, E.J. Delikatny, J.D. Glickson, M.A. Wasik, Decreased lactate concentration and glycolytic enzyme expression reflect inhibition of mTOR signal transduction pathway in B-cell lymphoma, NMR Biomed. 26 (1) (2012) 106–114.
[13] S.-C. Lee, H. Poptani, S. Pickup, W.T. Jenkins, S. Kim, C.J. Koch, E.J. Delikatny, J.D. Glickson, Early detection of radiation therapy response in non-Hodgkin's lymphoma xenografts by *in vivo*1H magnetic resonance spectroscopy and imaging, NMR Biomed. 23 (6) (2010) 624–632.
[14] H. Zhu, D. Rubin, Q. He, The fast spiral-SelMQC technique for in vivo MR spectroscopic imaging of polyunsaturated fatty acids in human breast tissue, Magnet. Reson. Med. 67 (1) (2012) 8–19.
[15] G. Melkus, P. Mörchel, V.C. Behr, M. Kotas, M. Flentje, P.M. Jakob, Sensitive J-coupled metabolite mapping using Sel-MQC with selective multi-spin-echo readout, Magnet. Reson. Med. 62 (4) (2009) 880–887.
[16] V.O. Boer, P.R. Luijten, D.W.J. Klomp, Refocused double-quantum editing for lactate detection at 7 T, Magnet. Reson. Med. 69 (1) (2012) 1–6.
[17] S. Thakur, J. Yaligar, J. Koutcher, In vivo lactate signal enhancement using binomial spectral-selective pulses in selective MQ coherence (SS-SelMQC) spectroscopy, Magnet. Reson. Med. 62 (3) (2009) 591–598.
[18] M. Murugananandham, J.A. Koutcher, G. Pizzorno, Q. He, In vivo tumor lactate relaxation measurements by selective multiple-quantum-coherence (Sel-MQC) transfer, Magnet. Reson. Med. 52 (4) (2004) 902–906.
[19] S. Magnitsky, G.K. Belka, C. Sterner, S. Pickup, L.A. Chodosh, J.D. Glickson, Lactate detection in inducible and orthotopic Her2/neu mammary gland tumours in mouse models, NMR Biomed. 26 (1) (2012) 35–42.
[20] J. Bell, J. Brown, G. Kubal, P. Sadler, NMR-invisible lactate in blood plasma, FEBS Lett. 235 (1) (1988) 81–86.
[21] M.S. Vinding, I.I. Maximov, Z. Tošner, N.C. Nielsen, Fast numerical design of spatial-selective rf pulses in MRI using Krotov and quasi-Newton based optimal control methods, J. Chem. Phys. 137 (5) (2012) 054203.
[22] N. Khaneja, T. Reiss, C. Kehlet, T. Schulte-Herbrüggen, S. Glaser, Optimal control of coupled spin dynamics: design of NMR pulse sequences by gradient ascent algorithms, J. Magnet. Reson. 172 (2) (2005) 296–305.
[23] T.E. Skinner, N.I. Gershenzon, M. Nimbalkar, W. Bermel, B. Luy, S.J. Glaser, New strategies for designing robust universal rotation pulses: application to broadband refocusing at low power, J. Magnet. Reson. 216 (0) (2012) 78–87.
[24] C.T. Kehlet, A.C. Sivertsen, M. Bjerring, T.O. Reiss, N. Khaneja, S.J. Glaser, N.C. Nielsen, Improving solid-state NMR dipolar recoupling by optimal control, J. Am. Chem. Soc. 126 (33) (2004) 10202–10203.
[25] Z. Tosner, T. Vosegaard, C. Kehlet, N. Khaneja, S.J. Glaser, N.C. Nielsen, Optimal control in NMR spectroscopy: numerical implementation in SIMPSON, J. Magnet. Reson. 197 (2) (2009) 120–134.
[26] G. Matson, K. Young, L. Kaiser, RF pulses for in vivo spectroscopy at high field designed under conditions of limited power using optimal control, J. Magnet. Reson. 199 (2009) 30–40.
[27] N. Boulant, D.L. Bihan, A. Amadon, Strongly modulating pulses for counteracting RF inhomogeneity at high fields, Magnet. Reson. Med. 60 (3) (2008) 701–708.
[28] N. Boulant, J. Mangin, A. Amadon, Counteracting radio frequency inhomogeneity in the human brain at 7 Tesla using strongly modulating pulses, Magnet. Reson. Med. 61 (5) (2009) 1165–1172.

[29] S. Conolly, D. Nishimura, A. Macovski, Optimal control solutions to the magnetic resonance selective excitation problem, IEEE Trans. Med. Imag. 5 (2) (1986) 106.
[30] I. Maximov, J. Salomon, G. Turinici, N. Nielsen, A smoothing monotonic convergent optimal control algorithm for nuclear magnetic resonance pulse sequence design, J. Chem. Phys. 132 (2010) 084107.
[31] I. Maximov, Z. Tošner, N. Nielsen, Optimal control design of NMR and dynamic nuclear polarization experiments using monotonically convergent algorithms, J. Chem. Phys. 128 (2008) 184505.
[32] A. Haase, J. Frahm, W. Hanicke, D. Matthaei, 1H NMR chemical shift selective (CHESS) imaging, Phys. Med. Biol. 30 (4) (1985) 341.
[33] P.-F. Van de Moortele, C. Akgun, G. Adriany, S. Moeller, J. Ritter, C.M. Collins, M.B. Smith, J.T. Vaughan, K. Ugurbil, B1 destructive interferences and spatial phase patterns at 7 T with a head transceiver array coil, Magnet. Reson. Med. 54 (6) (2005) 1503–1518.
[34] Y. Maday, G. Turinici, New formulations of monotonically convergent quantum control algorithms, J. Chem. Phys. 118 (2003) 8191.